



**HAL**  
open science

# On the Validity of the Asymptotic Near-Ground Propagation Model of Hertzian Dipole for Finite-Length Dipole Antennas

Hocine Belaid, Shermila Mostarshedi, Benoit Poussot, Jean-Marc Laheurte

► **To cite this version:**

Hocine Belaid, Shermila Mostarshedi, Benoit Poussot, Jean-Marc Laheurte. On the Validity of the Asymptotic Near-Ground Propagation Model of Hertzian Dipole for Finite-Length Dipole Antennas. IEEE Antennas and Wireless Propagation Letters, 2022, 21 (12), pp.1-5. 10.1109/LAWP.2022.3193581 . hal-03851418

**HAL Id: hal-03851418**

**<https://hal.science/hal-03851418>**

Submitted on 27 Mar 2023

**HAL** is a multi-disciplinary open access archive for the deposit and dissemination of scientific research documents, whether they are published or not. The documents may come from teaching and research institutions in France or abroad, or from public or private research centers.

L'archive ouverte pluridisciplinaire **HAL**, est destinée au dépôt et à la diffusion de documents scientifiques de niveau recherche, publiés ou non, émanant des établissements d'enseignement et de recherche français ou étrangers, des laboratoires publics ou privés.

# Extension of the asymptotic near-ground propagation model of Hertzian dipole to finite-length dipole antennas

Hocine Belaid\*, Shermila Mostarshedi, Benoit Poussot and Jean-Marc Laheurte

Univ Gustave Eiffel, CNRS, ESYCOM, F-77454 Marne la Vallée, France

E-mail\* : [hocine-anis.belaid@univ-eiffel.fr](mailto:hocine-anis.belaid@univ-eiffel.fr)

**Abstract**—This paper deals with the near-ground propagation of electromagnetic waves, when the emitting antenna is a finite length dipole, rather than an elementary one. The existing propagation model for an elementary Hertzian dipole is extended to a realistic case by assuming a known current distribution over the finite-length dipole. Validation of the theoretical models by an electromagnetic simulator (NEC2d) is also presented in this article.

**Index Terms**—Near-ground propagation model, finite-length dipole antennas, Vertical electric dipole.

## I. INTRODUCTION

Wireless sensor networks (WSN) have been widely deployed for environment and urban monitoring purposes. In some cases, sensors are placed close to a lossy interface in order to collect data of interest (e.g. precision agriculture or structural health monitoring of civil engineering infrastructures). Various measurement-based studies can be found to treat the near-ground wireless channel [1], [2]. More sophisticated physics-based yet easy-to-use propagation models for near-ground sensor networks are scarce [3], [4].

The radiation of a near-ground sensor may typically be handled by the famous Sommerfeld half-space problem. The Sommerfeld formulation is widely accepted in the community and can be validated by rigorous mathematical treatment [5]–[8]. However, the parameter manipulation for a link designer may be complicated using the accurate analysis of the problem and the associated Green's functions formalism [9]. The steepest descent technique can provide an asymptotic approximation of the field radiated by an elementary dipole over a lossy interface [10], [11].

In [12], authors have highlighted a region with an improved path loss for the near-ground link of an elementary Vertical Electric Dipole (VED). This region is bounded between two critical distances where the surface wave becomes predominant. Analytical expressions for the estimation of the two critical distances, i.e. the beginning and the end of the region of interest, have been obtained. Although the simple and ready-to-use expressions presented in this paper make the prediction of the wave propagation easier, yet the validity of them is not guaranteed for a finite-length antenna in a near-ground scenario.

In this paper, we propose an asymptotic extension for the near-ground propagation model of a VED seen in [12], in

order to adapt it to the finite-length dipole antenna. In section II, the problem of the near-ground link is described and the asymptotic extension of the VED problem to the case of finite-length Vertical Dipole (VD) is presented. Section III demonstrates the domain of validity of the extended model using the electromagnetic simulator NEC2d as reference. The critical distances for the VD case are estimated in section IV and are compared to those of the VED, followed by a complete parametric study, before concluding in section V.

## II. HALF-SPACE PROBLEM FOR VED AND VD

In this section, the well-know radiation model of an infinitesimal Vertical Electric Dipole (VED) over a lossy interface is reviewed and extended to obtain an asymptotic radiation model for a finite-length Vertical Dipole (VD) corresponding to a realistic antenna.

### A. Infinitesimal model

The Sommerfeld half-space problem for a Hertzian dipole invokes image theory. As we can see in Fig.1, the model of the problem is composed of an infinite lossy interface dividing the space into two different media, the source (VED) and the observation point being placed in medium 1. All the parameters of the model are summarised in Table 1. In such a scenario, the propagation is due to three wave components: the direct wave, the reflected wave and a third component namely the surface wave, due to the diffraction by the interface.

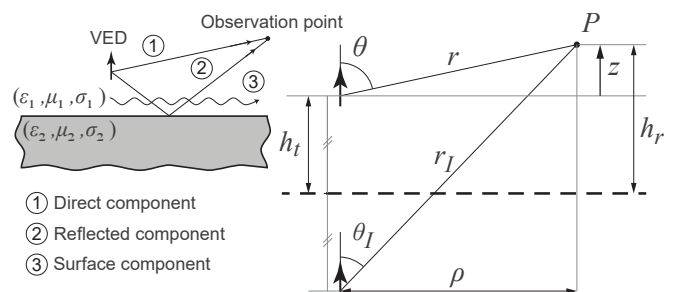


Fig. 1: Schematic of a VED radiating over a lossy half-space

TABLE I: Parameters of the problem

Param.	Description
$\delta l$	Infinitesimal length of VED
$h_t$	Height of VED
$h_r$	Height of observation point $P$
$\rho$	Radial distance between VED and observation point $P$
$z$	Vertical distance between VED and observation point $P$
$(\varepsilon_i, \mu_i, \sigma_i)$	Electromagnetic characteristics of propagation medium ( $i = 1$ ) and lossy medium ( $i = 2$ )

The radiated electric field of a VED over a lossy interface can be estimated with a good accuracy by its dominant component,  $E_z^{\text{VED}}$  [13]. As demonstrated in [12], the  $E_z^{\text{VED}}$  component of the electric field radiated by a VED over an interface is given by:

$$\begin{aligned}
E_z^{\text{VED}}(\rho, z) &= -jI_0\delta l\eta_1k_1 \left[ \sin^2(\theta) \frac{e^{-jk_1r}}{4\pi r} \right. \\
&\quad + \frac{\varepsilon_2jk_{z_1} - \varepsilon_1jk_{z_2}}{\varepsilon_2jk_{z_1} + \varepsilon_1jk_{z_2}} \sin^2(\theta_I) \frac{e^{-jk_1r_I}}{4\pi r_I} \\
&\quad - j \frac{1 - j\sqrt{\pi\tau}e^{-\tau}\text{erfc}(j\sqrt{\tau})}{\sqrt{\sin(\theta_I)[\cos(\omega_p - \theta_I) - 1]}} \\
&\quad \left. \times \sqrt{2\sin^7(\omega_p)} \frac{n^2}{1 - n^2} \cos(\omega_p) \frac{e^{-jk_1r_I}}{4\pi r_I} \right] \\
&= I_0\delta lf(\rho, z) \quad (1)
\end{aligned}$$

where the radiuses and angles  $(r, \theta)$  and  $(r_I, \theta_I)$  are functions of  $\rho$  and  $z$  which are related to the relative positions of the observation point  $P$ , the VED and the VED image (see Fig. 1).  $I_0\delta l$  is the dipolar moment of the VED,  $\eta_1$  is the medium impedance,  $k_1$  is the wavenumber,  $\omega_p = \arccos(\sqrt{\varepsilon_1/(\varepsilon_1 + \varepsilon_2)})$  is the pole of the reflection coefficient,  $n = \sqrt{\varepsilon_2/\varepsilon_1}$  is the refractive index provided that the first medium is vacuum, and  $\tau(\rho, z) = jk_1r_I[\cos(\omega_p - \theta_I) - 1]$  is the numerical distance [12].

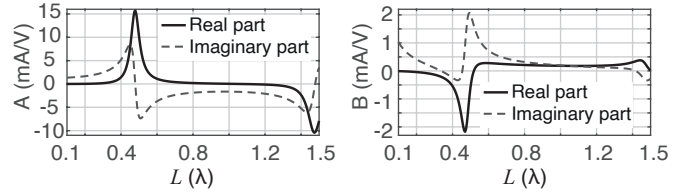
### B. Extension of the infinitesimal model

In order to adapt the infinitesimal model seen in (1) to a finite-length VD case, we assume that the VD of length  $L$  and radius  $a$  is composed of an infinite set of elementary dipoles, each one having an infinitesimal length of  $\delta l$  and a specific current value. This approach is legitimated by [14], where the author uses it to obtain the field components of a VD. The exact value of each current element is obviously unknown and needs to be calculated by a rigorous computational method such as the method of moments [15]. However, as a good approximation, the current distribution over a VD can be given by the Storer's variational method (valid for  $L/\lambda \in [0, 1.5]$ ) [16]. For a feeding voltage of 1V, the current distribution of a dipole centred at  $z' = 0$  has the following form:

$$I(z') = A \sin \left[ k_1 \left( \frac{L}{2} - |z'| \right) \right] + B \left( 1 - \cos \left[ k_1 \left( \frac{L}{2} - |z'| \right) \right] \right) \quad (2)$$

where  $z' \in [-L/2, L/2]$  defines the vertical position over the dipole, and  $A$  and  $B$  are complex coefficients varying according to the length and the radius of VD. The evolution

of these coefficients according to the VD normalised length and for a given form factor  $\Omega = 2 \ln(L/a)$  is drawn in Fig. 2:

Fig. 2: Storer's coefficients for a given form factor of  $\Omega = 15$ 

The total field  $E_z^{\text{VD}}$  radiated by the VD can be seen as the superposition of the fields  $E_z^{\text{VED}}$  of each VED [14]. The expression for  $E_z^{\text{VD}}$  is consequently given by :

$$E_z^{\text{VD}} = \int_{-L/2}^{+L/2} I(z')f(\rho, z - z')dz' \quad (3)$$

For a fair comparison of the fields radiated by an infinitesimal and a finite-length dipole, the dipolar moment of the VED is driven by calculating that of the VD. The right side of (4) provides the dipolar moment of the VD. The following equivalence can thus be obtained:

$$\begin{aligned}
I_0\delta l &= \int_{-L/2}^{+L/2} I(z')dz' \\
&= \frac{\lambda}{\pi} \left\{ A \left[ 1 - \cos\left(\frac{k_1L}{2}\right) \right] + B \left[ \frac{k_1L}{2} - \sin\left(\frac{k_1L}{2}\right) \right] \right\} \quad (4)
\end{aligned}$$

In the following sections, this equivalence is systematically applied to estimate the excitation current of VED.

### III. VALIDATION OF THE EXTENDED MODEL

In this section, we validate the extended model using NEC2d [17]. To this aim, two test configurations are considered, and their main parameters are summarised in Table II. The first configuration presents a typical example of sea-propagation and maritime radio-communications [18]. For the second configuration, the parameters have been chosen to achieve a near-ground wireless communication, where the ground has been coated by a layer of low-cost graphite [19] in order to possibly improve the path loss. The electric fields radiated by VED ( $E_z^{\text{VED}}$ ) and by VD obtained by the extended model ( $E_z^{\text{VD}}$ ) and by NEC2d ( $E_z^{\text{NEC}}$ ) are shown and compared in Fig. 3.

TABLE II: Test configurations

	f (MHz)	$h_t$ ( $\lambda$ )	$h_r$ ( $\lambda$ )	L ( $\lambda$ )	$\Omega$	$\varepsilon_r$	$\sigma_2$ (S/m)
Config. 1	5	1	1	0.25	10	81	5
Config. 2	2450	0.5	0.5	0.5	15	3	1e4

The figure shows that the extended model gives the same result as the infinitesimal model and presents a quasi-constant difference of less than 0.5 dB with the NEC2d simulation over a large interval of radial distances  $\rho$  in the far-field region. This difference is supposedly due to the Storer's current distribution

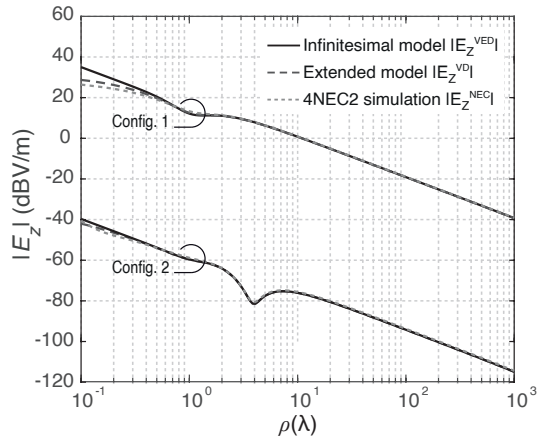


Fig. 3: Evolution of  $|E_z|$  as a function of the radial distance ( $\rho$ ) for both test configurations

which is valid for a dipole in free space and would be altered by the presence of the lossy interface.

Using an electromagnetic simulator, e.g. NEC2d, we are able to quantify the difference between the current distribution given by Storer's formulation (neglecting the interface) and obtained by NEC2d (including the interface). We also introduce  $\tilde{E}$  (dB), which is the maximum error between the electric fields obtained by NEC2d (NEC2d current) and the extended model (Storer's current) in far-field for distances varying up to  $1e3\lambda$ . Table III summarises the parameters for a worst case scenario of a PEC interface and Fig.4 shows the results accordingly.

TABLE III: Parameters for current distribution

f (MHz)	L ( $\lambda$ )	$h_t - L/2$ ( $\lambda$ )	$\Omega$	$\epsilon_r$	$\sigma_2$ (S/m)
2450	0.25		15	1	$\rightarrow \infty$
	0.50	0.00025 ( $\rightarrow 0$ )			
	0.75	50 ( $\rightarrow \infty$ )			
	1.00				

These results show that the closer to the interface the dipole is, the more the NEC2d current distribution differs from the Storer's estimation, as it becomes more asymmetric. According to Fig. 4, the error for the worst case presenting a resonant dipole very close to a PEC interface ( $L = \lambda/2$ ,  $h_t - L/2 \rightarrow 0$  and  $\sigma \rightarrow \infty$ ) is equal 3.79 dB.

#### IV. CRITICAL DISTANCES

In order to locate and quantify the impact of the surface component on the radiated field, we introduce the critical distances, given by  $\rho_{\min}$  and  $\rho_{\text{break}}$ . In a near-ground communication link, the main goal of these two distances is to identify the region where the surface component is predominant.

##### A. Definitions

The critical distances can be determined in different ways. In [5], [11], [12] analytical expressions for the critical distances in the case of an elementary VED are obtained subsequent to a few approximations:

$$\rho_{\min} = |n|(h_t + h_r) \quad \rho_{\text{break}} = \frac{2|n^2|}{k_1} \quad |n^2| > 10 \quad (5)$$

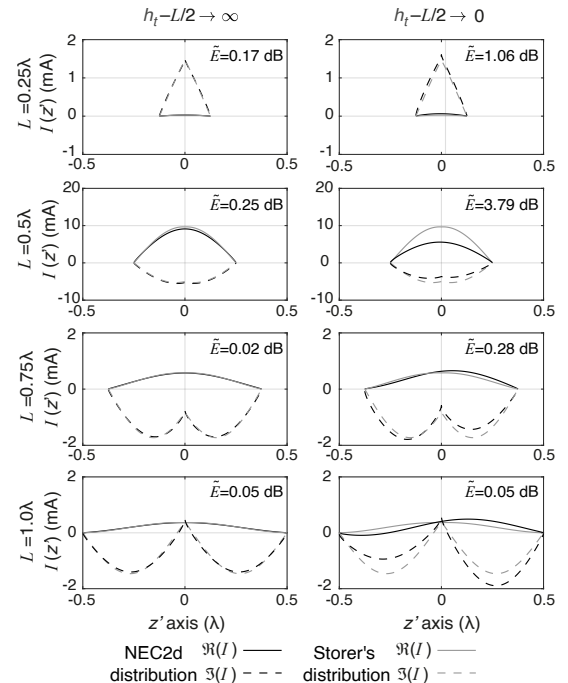


Fig. 4: Currents distributions according to different parameters

where  $\rho_{\min}$  is also the distance at which the reflection coefficient of the interface is minimum and  $\rho_{\text{break}}$  (also known as  $\rho_{\text{knee}}$  in [5]) is the distance at which the Sommerfeld numerical distance ( $|\tau|$ ) is close to unity. These two concepts are tightly related to a VED and without any new proof, are not applicable in the case of a VD.

Therefore, in this paper, we introduce a more generic definition for the critical distances, in order to be used for both VD and VED. We define  $\rho_{\min}$  as the distance from which the surface component becomes predominant compared to the other components ( $|E_z \text{ surface}| > |E_z \text{ direct+reflected}|$ ), and  $\rho_{\text{break}}$  as the distance at which the surface component reaches its maximum amplitude ( $|E_z \text{ surface}| \rightarrow |E_z \text{ surface}|_{\max}$ ). For the two configurations in Table II, both  $E_z^{\text{VD}}$  and  $E_z^{\text{VED}}$  are compared in Fig. 5 with the two-ray method [20], which excludes the surface component.

Fig. 5 brings into focus a substantial difference between the two-ray method and the infinitesimal ( $E_z^{\text{VED}}$ ) and extended ( $E_z^{\text{VD}}$ ) models. We define the region of interest to be the range of  $\rho$  distances between  $\rho_{\min}$  and  $\rho_{\text{break}}$ , where the infinitesimal and extended models show noticeable improvement compared to the two-rays method, provided that the conditions over the frequency, the heights and the interface conductivity are fulfilled [12]. We define  $\Delta E_z$  as the maximum difference between the two-ray method and the infinitesimal/extended models, which by definition occurs at  $\rho_{\text{break}}$ . Table IV summarises the outputs of the infinitesimal and extended models for the two configurations of Fig. 5 and shows an excellent agreement between them. In order to rule on the equivalence between the infinitesimal and the extended models, beyond these two specific configurations, a parametric study is performed in the next subsection.

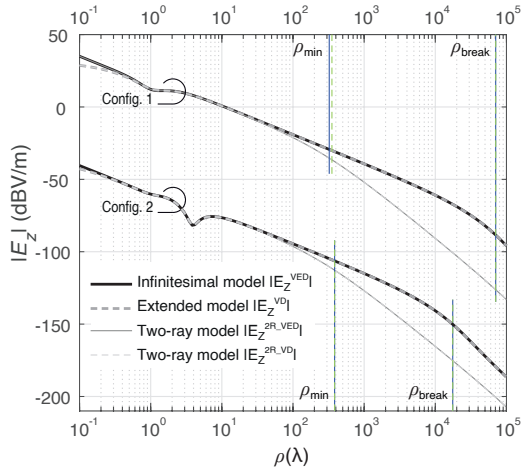


Fig. 5: Evolution of  $|E_z|$  for different models and the associated critical distances for both test configurations

TABLE IV: Infinitesimal and extended model outputs

	$\rho_{\min}$ ( $\lambda$ )		$\rho_{\text{break}}$ ( $\lambda$ )		$\Delta E_z$ (dB)	
	VED	VD	VED	VD	VED	VD
Config. 1	4.08e3	4.45e3	5.77e5	5.77e5	34.3	34.3
Config. 2	6.41	6.41	2.93e2	2.93e2	25.5	25.5

### B. Parametric study

In this section, a parametric study is performed for both infinitesimal and extended models by varying the height of the dipole  $h_t$ , the frequency  $f$ , the interface conductivity  $\sigma$  and the dipole length  $L$ . The outputs of the two models, i.e.  $\rho_{\min}$ ,  $\rho_{\text{break}}$  and  $\Delta E_z$ , are compared. The goal is to rule on the validity of the infinitesimal model for a finite-length dipole. All the cases and input parameters are summarised in Table V, and the results are illustrated in Fig. 6.

TABLE V: Description of the parametric study

	Case 1	Case 2	Case 3	Case 4
$h_t$ ( $\lambda$ )	[0.125, 2]	1	1	1
$f$ (MHz)	5	[1, 100]	5	5
$\sigma$ (S/m)	5	5	[0.1, 10]	5
$L$ ( $\lambda$ )	0.25	0.25	0.25	[0.25, 1]
$\epsilon_r$	81	81	81	81
$h_r$ ( $\lambda$ )	1	1	1	1

Fig. 6 shows that the evolution of the outputs of both models are almost identical, the curves being overlapped for all cases and over all the distances. Case 1 shows that by increasing the height of the dipole  $h_t$ ,  $\rho_{\min}$  increases and  $\rho_{\text{break}}$  stays constant. Consequently, the region of interest shrinks as the heights increase and the contribution of the surface component reduces as  $\Delta E_z$  decreases. Case 2 shows that the critical distances as well as the contribution of the surface component decrease by increasing the frequency. Contrarily, in case 3, the critical distances as well as the contribution of the surface component increase by increasing the conductivity of the interface. Finally, case 4 shows that the normalised dipole length  $L$  has no influence on the models' outputs.

In summary, by increasing the height of the dipole  $h_t$ , and

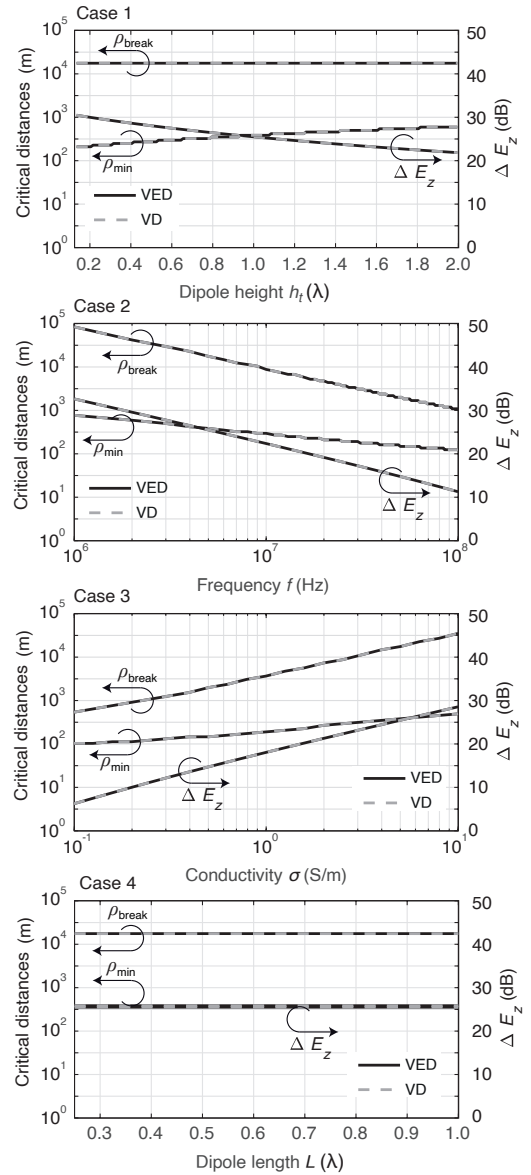


Fig. 6: Evolution of output parameters for four studied cases

the frequency  $f$ , the zone of improved path loss and  $\Delta E_z$  are reduced, while by increasing the conductivity of the interface  $\sigma$ , the zone of interest and  $\Delta E_z$  are further improved.

### V. CONCLUSION

In this paper, we took the elementary VED above a conductive half-space as reference and ruled on the validity of the infinitesimal model for the finite-length dipole. An extension of the infinitesimal model has been proposed and used through different studies. This extended model, provided with the Storer's current distribution, matches closely with the results given by NEC2d.

On the basis of the results reported in section III and IV, we can claim that the infinitesimal model and its critical distances given in (5) are still valid for a finite-length VD and, more importantly, we are able to state that a VED shows the same field-evolution as a VD, and can rigorously substitute it in the context of the Sommerfeld half-space problem.

## REFERENCES

- [1] S. Duan, R. Su, C. Xu, Y. Chen, and J. He, "Ultra-wideband radio channel characteristics for near-ground swarm robots communication," *IEEE Transactions on Wireless Communications*, vol. 19, no. 7, pp. 4715–4726, 2020.
- [2] M. Aslam and S. A. Zekavat, "New channel path loss model for near-ground antenna sensor networks," *IET Wireless Sensor Systems*, vol. 2, no. 2, pp. 103–107, 2012.
- [3] A. Torabi and S. A. Zekavat, "A rigorous model for predicting the path loss in near-ground wireless sensor networks," in *2015 IEEE 82nd Vehicular Technology Conference (VTC2015-Fall)*. IEEE, 2015, pp. 1–5.
- [4] W. Tang, X. Ma, J. Wei, and Z. Wang, "Measurement and analysis of near-ground propagation models under different terrains for wireless sensor networks," *Sensors*, vol. 19, no. 8, p. 1901, 2019.
- [5] K. Michalski and J. Mosig, "The sommerfeld half-space problem revisited: from radio frequencies and zenneck waves to visible light and fano modes," *Journal of Electromagnetic Waves and Applications*, vol. 30, no. 1, pp. 1–42, 2016.
- [6] R. W. King, *The Theory of Linear Antennas*. Harvard University Press, 1956.
- [7] K. Sivaprasad, "An asymptotic solution of dipoles in a conducting medium," *IEEE Transactions on Antennas and Propagation*, vol. 11, no. 2, pp. 133–142, 1963.
- [8] W. C. Chew, *Lectures on Electromagnetic Field Theory*. Purdue University, 2019.
- [9] D. Liao and K. Sarabandi, "Near-earth wave propagation characteristics of electric dipole in presence of vegetation or snow layer," *IEEE Transactions on Antennas and Propagation*, vol. 53, no. 11, pp. 3747–3756, 2005.
- [10] R. W. King, "Electromagnetic field of a vertical dipole over an imperfectly conducting half-space," *Radio Science*, vol. 25, no. 2, pp. 149–160, 1990.
- [11] K. Michalski and J. Mosig, "The sommerfeld halfspace problem redux: Alternative field representations, role of zenneck and surface plasmon waves," *IEEE Transactions on Antennas and Propagation*, vol. 63, no. 12, pp. 5777–5790, 2015.
- [12] M. H. B. Cardoso, S. Mostarshedi, G. Baudoin, and J.-M. Laheurte, "Analytical expressions of critical distances for near-ground propagation," *IEEE Transactions on Antennas and Propagation*, vol. 66, no. 5, pp. 2482–2493, 2018.
- [13] T. Alves, B. Poussot, and J.-M. Laheurte, "Analytical propagation modeling of BAN channels based on the creeping-wave theory," *IEEE Transactions on Antennas and Propagation*, vol. 59, no. 4, pp. 1269–1274, 2010.
- [14] C. A. Balanis, *Antenna theory: analysis and design*. John Wiley & sons, 2015.
- [15] W. C. Gibson, *The method of moments in electromagnetics*. Chapman and Hall/CRC, 2021.
- [16] J. E. Storer, "Variational solution to the problem of the symmetrical cylindrical antenna," *Office of Naval Research*, no. 101, 1950.
- [17] G. J. Burke and A. J. Poggio, "Numerical electromagnetics code (nec) - method of moments," *Lawrence Livermore Laboratory*, 1981.
- [18] R. ITU, "Electrical characteristics of the surface of the earth," *ITU-R P. 523-7*, 1992.
- [19] C. A. Balanis and D. DeCarlo, "Monopole antenna patterns on finite size composite ground planes," *IEEE Transactions on Antennas and Propagation*, vol. AP-30, no. 4, pp. 764–768, 1982.
- [20] S. S. Haykin and M. Moher, *Modern wireless communications*. Pearson Education India, 2011.